nature communications

Article

https://doi.org/10.1038/s41467-025-67909-9

bZIP factors of the Unfolded Protein Response interact with PIF4 to promote thermomorphogenesis

Received: 29 May 2025

Accepted: 11 December 2025

Published online: 30 December 2025

Check for updates

Dan Zhang, Haiying Xu & Nam-Hai Chua

When Arabidopsis plants are exposed to warm temperatures (e.g., 29 °C), they undergo adaptive growth known as thermomorphogenesis. This process is primarily regulated by the phytochrome B (phyB)-PHYTOCHROME-INTERACTING FACTOR 4 (PIF4) module; however, the potential involvement of additional signaling pathways remains underexplored. Here, we show that warmth triggers endoplasmic reticulum (ER) stress, activating both arms of the Unfolded Protein Response (UPR). Three UPR-associated bZIP transcription factors, bZIP17, bZIP28 and bZIP60, promote hypocotyl growth under warmth in a PIF4-dependent manner. Active bZIP factors form complexes with PIF4 in the nucleus, where they bind to promoter regions of *PIF4* and other growth-related genes to enhance their expression. In parallel, bZIPs overexpression counteract the inhibitory effect of phyB on PIF4 stability, thereby reinforcing thermomorphogenic growth. Together, our findings define a regulatory axis that links ER stress, the UPR and thermomorphogenesis, clarifying how plants coordinate physiological and environmental cues to adapt to warming conditions.

Plants are constantly being exposed to environmental stressors that disrupt cellular functions leading to impaired growth and reduced productivity[1–3]. One essential mechanism for mitigating stress-induced damage is the Unfolded Protein Response (UPR), a conserved signaling pathway that alleviates endoplasmic reticulum (ER) stress caused by the accumulation of misfolded proteins under stress conditions[4,5]. In plants, the UPR is primarily regulated by three BASIC LEUCINE ZIPPER (bZIP) transcription factors, bZIP17, bZIP28, and bZIP60. In response to ER stress, bZIP17 and 28 undergo proteolytic processing, while *bZIP60* mRNA undergoes IRE1-dependent unconventional splicing, leading to the generation of active forms of bZIP factors–bZIP17N, bZIP28N, and bZIP60s, which translocate to the nucleus to regulate expression of stress-responsive genes[4–7].

Heat stress is a well-known inducer of ER stress, disrupting protein homeostasis and, subsequently, activating the UPR[8–13]. Priming-mediated thermotolerance at 37 °C further demonstrates the involvement of UPR components[14]; however, whether moderately elevated temperatures also induce ER stress remains unclear. Thermomorphogenesis, an adaptive growth response to moderately elevated temperatures (e.g., 29 °C), is primarily regulated by PHYTOCHROME-INTERACTING FACTOR 4 (PIF4), which controls the expression of growth-related genes[15–17]. Given that thermomorphogenesis requires increased synthesis of secreted proteins for cell elongation, moderate temperature stress may impose additional pressure on the ER, raising the possibility that UPR signaling may contribute to thermomorphogenesis.

Results

Warm temperature rapidly activates UPR signaling prior to induction of canonical thermoresponsive genes

To determine whether elevated ambient growth temperatures would trigger UPR, we exposed Arabidopsis seedlings to 29 °C (warmth) and analyzed gene expression levels at multiple time intervals. Figure 1a shows that in a short-term kinetic assay, *bZIP28* transcripts increased within 20 min upon warmth treatment, followed by the elevated expression of UPR marker *BiP1* at 30 min (Fig. 1b). *PIF4* transcripts were

Temasek Life Sciences Laboratory, National University of Singapore, Singapore, Singapore. e-mail: chua@rockefeller.edu

https://doi.org/10.1038/s41467-025-67909-9

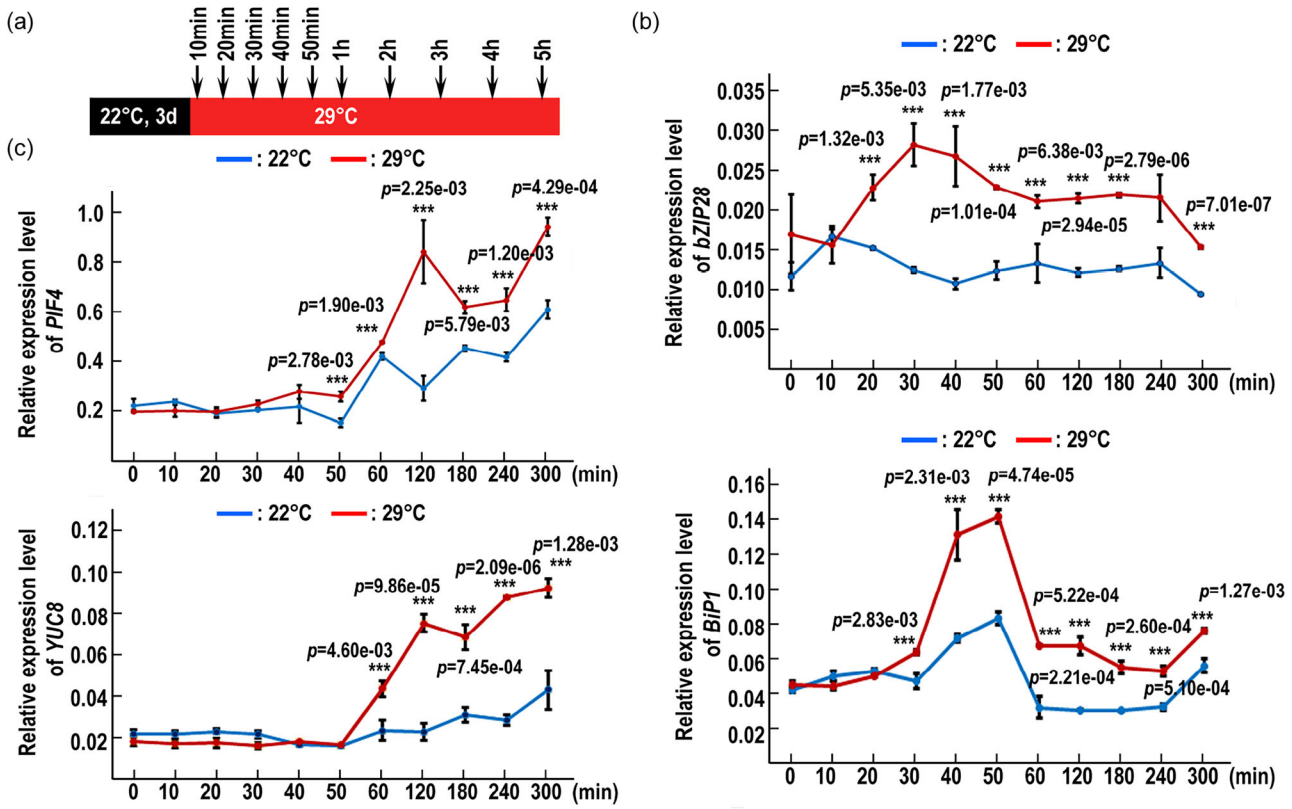

Fig. 1 | Short-term warm temperature activates the Unfolded Protein Response (UPR) in Arabidopsis. a Schematic illustration of experimental design. Wild-type (WT) seedlings were grown at 22 °C for 3 days and then transferred to 29 °C for the indicated time points. Control seedlings were maintained at 22 °C. Relative expression levels of UPR-related genes (*bZIP28* and *BiP1*, **b**) and warmth-responsive genes (*PIF4* and *YUC8*, **c**) in the samples from the experimental setup shown in (**a**). Gene expression was quantified via qRT-PCR and normalized to that of *actin* which serves as a reference. The error bars represent the s.d. ($n = 3$ biological replicates), and the centers of the error bars indicate the mean. Asterisks indicate significant differences between 22 °C and 29 °C-grown samples (unpaired two-sided *t*-test; ***P-value < 0.01).

subsequently induced at 50 min, with activation of the PIF4 target gene *YUCCA8* (*YUC8*) observed at a later time point, 60 min (Fig. 1c). In support of these findings, analysis of a previously published RNA-seq dataset revealed that *bZIP28* transcript abundance also increased within 20–30 min of warm treatment, whereas *PIF4* induction was detected only after 30 min[18], consistent with the temporal pattern we observed. These results indicate that UPR signaling is engaged earlier than the induction of canonical thermoresponsive genes during the transition to warm conditions.

To assess whether UPR activation is maintained over longer periods, transcript levels were monitored at extended time points (5 h to 13 d; Supplementary Fig. 1a). *BiP1* and *bZIP28* transcripts remained elevated under prolonged warmth, and spliced *bZIP60* (*bZIP60s*) transcripts were also induced, indicating activation of the second major UPR signaling branch (Supplementary Fig. 1b). This observation is reminiscent of that found with *PIF4* and *YUCCA8* (*YUC8*) genes (Supplementary Fig. 1c). Notably, the active nuclear form of bZIP28 (bZIP28N) was clearly detected by immunoblotting after 2 days of warmth treatment, but not under normal conditions (Supplementary Fig. 1d). Collectively, these findings demonstrate that warm temperature induce ER stress, rapidly activates UPR signaling ahead of *PIF4* and *YUC8* induction, and that this activation is sustained during prolonged exposure, suggesting an early involvement of UPR in thermomorphogenic growth.

Mild pharmacological ER stress promotes hypocotyl elongation in a PIF4-dependent manner

Activation of UPR signaling induced by pharmacological agents, including treatment with tunicamycin (Tm) and dithiothreitol (DTT), often results in strong seedling growth arrest and chlorosis, possibly due to drug overdose, which is in stark contrast to the growth-promoting effects of thermomorphogenesis. We therefore examined the effects of low Tm dosage on hypocotyl elongation, which is the most prominent and widely used marker for seedlings thermomorphogenesis. Arabidopsis seedlings were treated with 8 μg/L Tm, 10 times lower than the working concentration commonly used to induce acute ER stress (Supplementary Fig. 2a). Intriguingly, at this mild dose, seedlings displayed a modest but statistically significant increase in hypocotyl lengths at 22 °C, and such effect was further enhanced at 29 °C (Supplementary Fig. 2b, c). *BiP1* transcripts accumulated in Tm-treated seedlings compared to DMSO controls at 0 and 2 d under both temperature conditions, while *bZIP28* expression was significantly upregulated at 1 d under normal condition, and 2 d under warmth (Supplementary Fig. 2d, e). Notably, compared to normal temperature condition, *BiP1* and *bZIP28* transcripts accumulation increased at 29 °C, further supporting our observations that elevated temperature enhances ER stress. Together with the longer hypocotyls observed in Tm-treated seedlings at 29 °C relative to 22 °C, these results suggest a functional interplay between UPR signaling and thermomorphogenesis.

Since PIF4 functions as a central regulator of plant thermomorphogenesis through activating warmth-responsive gene expression, we examined its involvement in UPR-mediated growth regulation. Hypocotyl elongation induced by modest Tm treatment was abolished in *pif4* seedlings at either 22 °C or 29 °C (Supplementary Fig. 2b, c), indicating that Tm-induced UPR promotes hypocotyl elongation in a PIF4-dependent manner.

To determine whether PIF4 itself is involved in UPR regulation, we examined ER stress response of *pif4*. No significant differences in shoot or root growth were observed between *pif4* and WT seedlings upon Tm treatment (Supplementary Fig. 3a, b). Furthermore, analysis of UPR marker genes (*BiP1* and *BiP3*) showed comparable transcriptional response to Tm treatment between *pif4* and WT seedlings (Supplementary Fig. 3c). These results exclude the possibility of a defective UPR signalling in *pif4*.

Next, we examined whether the warmth-induced transcriptional activation of UPR signaling is regulated by PIF4. Notably, whereas *pif4* was completely insensitive to warmth treatment in terms of hypocotyl elongation, the transcriptional upregulation of *BiP1* and *bZIP28* in *pif4* was similar to that in WT seedlings under both short-term and prolonged warm treatments (Supplementary Fig. 4a, b). This finding suggests that warmth-induced activation of UPR signaling is independent of PIF4 regulation and likely functions upstream of PIF4 signaling.

bZIP factors of UPR promote thermomorphogenesis

Given that UPR-associated *bZIPs* are transcriptionally responsive to warmth, we next examined their roles in thermomorphogenesis. Single knockout mutants of *bzip17*, *bzip28*, *bzip60* exhibited no significant differences in hypocotyl lengths compared to WT at either 22 °C or 29 °C (Fig. 2a, b). Remarkably, at warmth, double mutants *bzip17/60* and *bzip28/60* displayed significantly shorter hypocotyl compared to WT, whereas remaining indistinguishable from WT at 22 °C (Fig. 2a, b). This suggests that the bZIP factors derived from both arms of the UPR pathway function alone or in concert with other factors to promote plant thermomorphogenic hypocotyl growth. In line with impaired hypocotyl elongation induced by warmth, *YUC8* and *PIF4* transcript levels were reduced in *bzip17/60* and *bzip28/60* double mutants compared to WT (Fig. 2c, d).

To further corroborate the positive roles of bZIP17, bZIP28 and bZIP60 in regulating thermomorphogenesis, we generated gain-of-function mutants overexpressing either the full-length or nuclear form of individual bZIPs in WT background. Compared to WT, both full-length and nuclear bZIPs-OE displayed enhanced hypocotyl elongation under warmth (Supplementary Fig. 5a, b, and 6, and Fig. 2e, f). In line with previously observed defects in thermomorphogenic hypocotyl growth in *bzip* loss-of-function mutants, warmth-induced hypocotyl elongation and marker gene expression were significantly enhanced in overexpression lines with no observable growth alteration at 22 °C (Fig. 2g, h).

The difference in hypocotyl lengths between *bzip17/60*, *bzip28/60* double mutants and *pif4* prompted us to further investigate the functional relationship between bZIPs and PIF4 during thermomorphogenesis. To this end, we crossed the double mutants with *pif4*. At warmth, the intermediate hypocotyl lengths of the double mutants were reduced to those of *pif4* in the *bzip17/60/pif4* and *bzip28/60/pif4* triple mutants (Fig. 2a, b). We further generated bZIP OE lines in *pif4* mutant background by crossing bZIP17N-OE, bZIP28N-OE or bZIP60s-OE lines with *pif4*. Western blot analysis confirmed bZIP protein levels in the *OE/pif4* lines were comparable to those in the WT background (Supplementary Fig. 6d). Interestingly, compared to the bZIP overexpression in WT background, hypocotyl elongation in the *OE/pif4* lines were insensitive to warmth, a phenotype similar to that of *pif4* (Fig. 2g, h). Together, these results indicate that PIF4 is required for bZIP-mediated promotion of thermomorphogenesis.

To further corroborate these observations, we generated double overexpression lines (bZIP28N/60s-OE and bZIP17N/60s-OE) in both WT and *pif4* background by genetic crosses. Neither bZIP28N/60s-OE/WT nor bZIP17N/60s-OE/WT displayed additional increased hypocotyl elongation compared to the single bZIP-OE line. These results suggest that bZIP17, bZIP28 and bZIP60 function in a shared pathway to regulate thermomorphogenesis (Supplementary Fig. 5c, d). Furthermore, bZIP28N/60s-OE/*pif4* and bZIP17N/60s-OE/*pif4* failed to rescue the *pif4* growth defect, confirming that UPR-mediated regulation of thermomorphogenesis is PIF4-dependent.

bZIP active forms, bZIP17N, bZIP28N and bZIP60s, interact with PIF4 in the nucleus and bZIP/PIF4 complexes are bound to promoter regions of PIF4-target genes

Since the thermomorphogenic growth mediated by UPR-bZIPs requires PIF4 functions, we hypothesized that the bZIP factors might function in a protein complex with PIF4 to regulate expression of downstream growth-promoting genes. Under ER stress conditions, the N-terminal domains of bZIP17 and bZIP28, along with bZIP60s, are translocated to the nucleus. We observed that the active forms of bZIPs co-localized with PIF4 in nuclei when transiently overexpressed in *Nicotiana benthamiana* (hereafter Nicotiana, Supplementary Fig. 7a). Quantitative colocalization analysis further supported this overlap, with Pearson correlation coefficients of ~0.5, indicating a nuclear co-localization between bZIP active forms and PIF4 (Supplementary Fig. 7b).

To examine whether there are direct interactions between bZIPs and PIF4, we performed in vitro pull-down assays using recombinant maltose binding protein (MBP)-tagged PIF4 and mCherry-tagged bZIP active forms. We found that PIF4 directly interacted with bZIP17N, bZIP28N, and bZIP60s but not with the mCherry negative control (Fig. 3a). In vivo associations were confirmed by co-immunoprecipitation (Co-IP) assays, wherein PIF4-flag co-immunoprecipitated with bZIP17N-HA and bZIP28N-HA, while PIF4-myc was co-immunoprecipitated by bZIP60s-flag in planta (Fig. 3b). In addition, PIF4-myc also co-immunoprecipitated with bZIP17N-HA, bZIP28N-HA (Supplementary Fig. 8). Intriguingly, we observed similar patterns under warmth condition, indicating that PIF4-bZIP complexes are preformed and maintained upon warming (Fig. 3b and Supplementary Fig. 8). In addition, results of Bimolecular fluorescence complementation (BiFC) assays in Nicotiana suggest that the active form of bZIPs interact with PIF4 in nuclei. Strong GFP fluorescence was detected in nuclei when PIF4-GFP^{C} was co-expressed with GFP^{N}-bZIP17N, GFP^{N}-bZIP28N, or GFP^{N}-bZIP60s whereas no signal was detected with the free GFP^{N} (Fig. 3c). Taken together, these results suggest that the active forms of UPR-associated bZIPs directly interact with PIF4 in Arabidopsis nuclei. This finding is consistent with previous reports showing that bZIP transcription factors interact with bHLH proteins[19,20].

Under warmth conditions, PIF4 directly targets multiple growth-promoting genes including *PIF4* itself to regulate thermomorphogenic growth[17,21]. To investigate whether bZIPs also bind to the promoter regions of PIF4-targeted warmth-responsive genes, we performed electrophoretic mobility shift assays (EMSA) using a DNA probe from the *PIF4* promoter region. bZIP17N, bZIP28N, bZIP60s protein specifically interacted with the G-box element within the *PIF4* promoter, forming distinct protein-DNA complexes (Fig. 3d). These associations were strongly reduced with the addition of a 100-fold molar excess of non-labeled G-box probes as a competitor and bindings were abolished when the G-box probes were mutated, consistent with previous reports that bZIP transcription factors can bind G-box elements in gene promoters[17,22]. These results indicate that bZIP proteins directly associate with the *PIF4* promoter region.

To confirm the binding in vivo, we performed chromatin immunoprecipitation (ChIP)-qPCR assays. bZIP17N, bZIP28N and bZIP60s were specifically enriched at the promoter regions of various PIF4-targeted genes, *PIF4*, *YUC8*, and *IAA19* (Fig. 3e–g). Although a weak enrichment of bZIPs at target promoters were detectable at 22 °C compared with the WT control, this basal binding was consistent with our EMSA results. Notably, such binding was markedly stronger at 29 °C, indicating that bZIPs association with these promoters is specifically enhanced under warmth.

https://doi.org/10.1038/s41467-025-67909-9

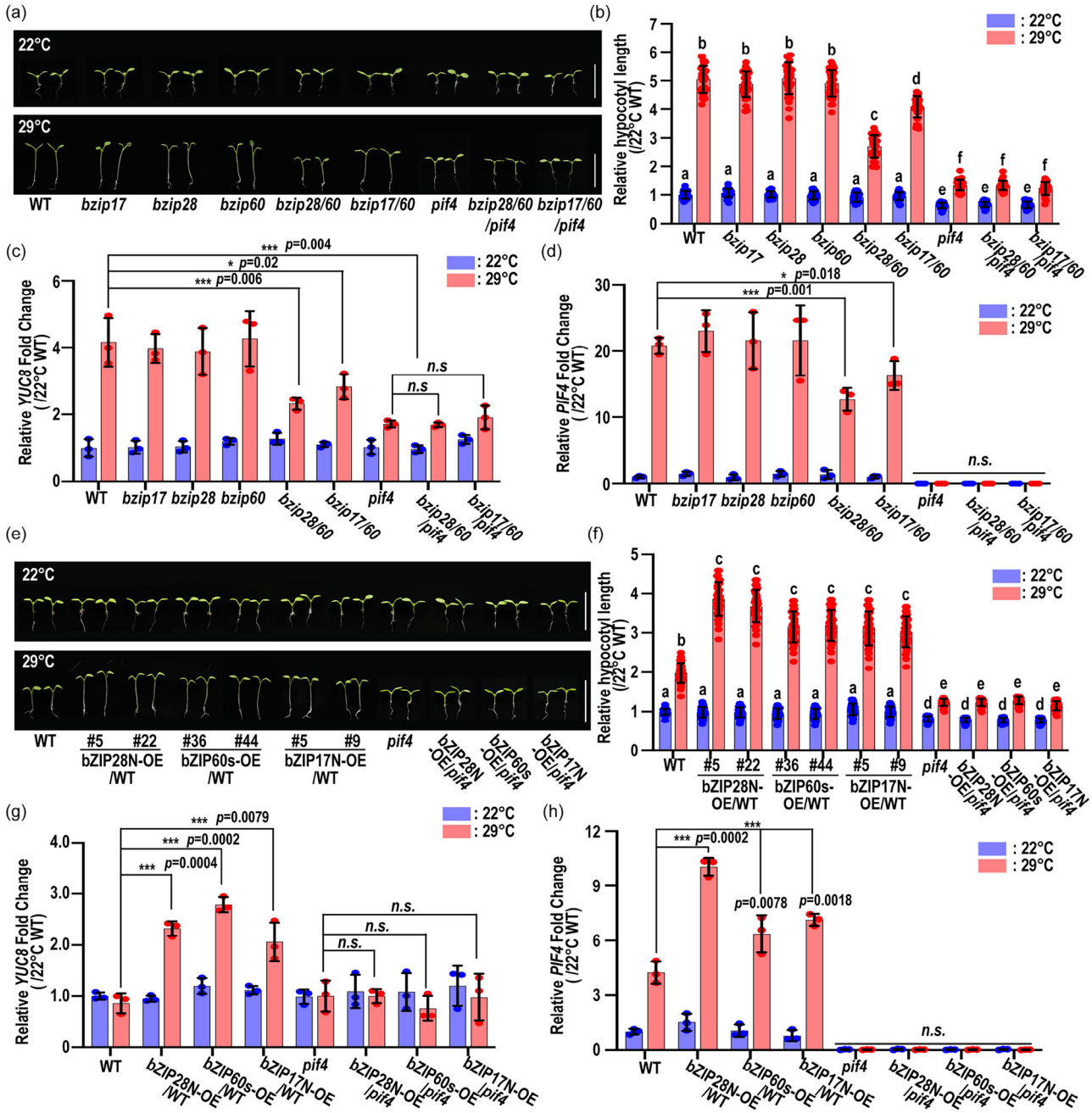

Fig. 2 | bZIP transcription factors promote thermomorphogenesis in a PIF4-dependent manner. a Representative images of 7-day-old WT, *pif4*, single (*bzip17*, *bzip28*, *bzip60*), double (*bzip28/60*, *bzip17/60*), and triple (*bzip28/60/pif4*, *bzip17/60/pif4*) mutants grown at 22 °C or 29 °C. Scale bar, 1 cm. **b** Hypocotyl lengths of seedlings shown in (**a**), normalized to WT at 22 °C (1.9 mm). The error bars represent the s.d. (n = 33 biological replicates), and the centers of the error bars indicate the mean. Different lowercase letters represent statistically significant differences (one-way ANOVA, Tukey's test, $P < 0.05$). Relative expression levels of thermo-responsive genes *YUC8* (**c**) and *PIF4* (**d**) in *bzip* mutants at 22 °C or 29 °C. Expression levels were normalized to those of *actin* which served as an internal control and with WT expression levels at 22 °C set to 1. The error bars represent the s.d. (n = 3 biological replicates), and the centers of the error bars indicate the mean. Asterisks indicate significant differences between 22 °C and 29 °C-grown samples (unpaired two-sided t-test; *P-value < 0.05; ***P-value < 0.01; *n.s.*, no significant difference). **e** Representative images of 5-day-old WT, *pif4*, bZIP nuclear form overexpression lines in either WT background (bZIP28N-OE/WT, bZIP60S-OE/WT, bZIP17N-OE/WT) or *pif4* background (bZIP28N-OE/*pif4*, bZIP60S-OE/*pif4*, bZIP17N-OE/*pif4*) grown at 22 °C or 29 °C. Scale bar, 1 cm. **f** Hypocotyl lengths of seedlings shown in (**e**), normalized to WT at 22 °C (1.3 mm). The error bars represent the s.d. (n = 33 biological replicates), and the centers of the error bars indicate the mean. Different lowercase letters represent statistically significant differences (one-way ANOVA, Tukey's test, $P < 0.05$). Relative expression levels of *YUC8* (**g**) and *PIF4* (**h**) in bZIPs-OE *lines* at 22 °C or 29 °C, normalized to those of *actin* (WT expression levels at 22 °C set as 1). The error bars represent the s.d. (n = 3 biological replicates), and the centers of the error bars indicate the mean. Asterisks indicate significant differences between 22 °C and 29 °C-grown samples (unpaired two-sided t-test; ***P-value < 0.01; *n.s.*, no significant difference).

Consistent with the observation that thermomorphogenic growth promoted by UPR-associated bZIPs requires PIF4 functions, the association of bZIPs with promoters of PIF4 target genes was significantly reduced and failed to display the warmth-induced binding activity in the absence of PIF4 (Fig. 3e–g). These results suggest that PIF4 is essential for the recruitment of bZIPs to the target gene promoters. Collectively, these findings indicate that bZIPs and PIF4 form a regulatory complex to

https://doi.org/10.1038/s41467-025-67909-9

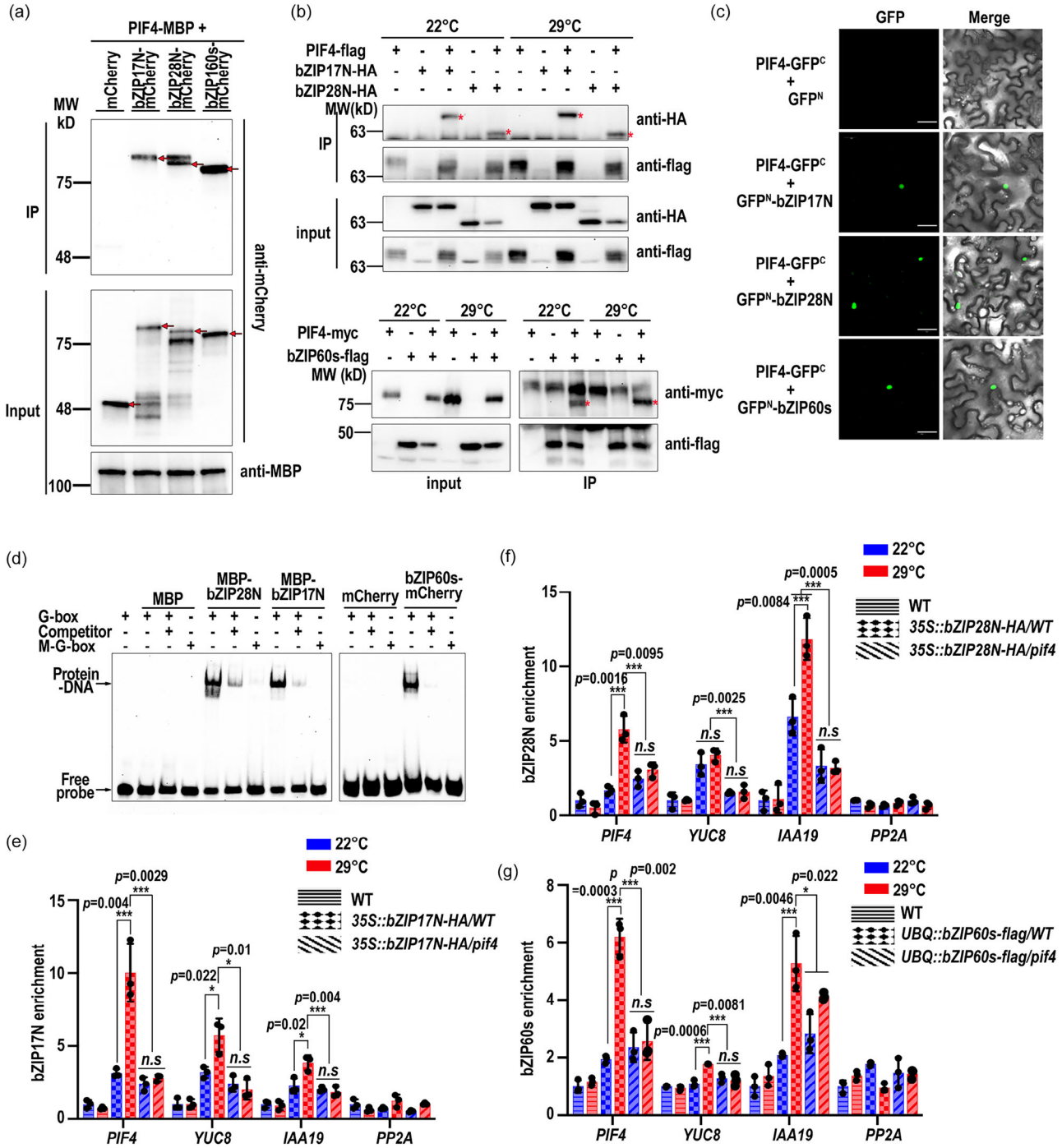

orchestrate expression of growth-promoting genes during thermomorphogenesis.

bZIP factors enhance PIF4 protein stability during thermomorphogenesis

PIF4 function is regulated by temperature at both transcriptional and posttranslational levels, and PIF4 protein stability is crucial for modulating warmth response of plants[17]. We found that warmth-induced transcriptional upregulation of *PIF4* was significantly reduced in *bzip* mutants, correlating with a strong reduction in PIF4 levels upon warm treatment (Supplementary Fig. 9a). In line with the enhanced thermomorphogenic growth observed in bZIP overexpression plants, *PIF4* transcript levels were highly upregulated when active form of UPR-associated bZIPs were overexpressed resulting in a greater PIF4 protein abundance (Supplementary Fig. 9b).

To determine whether bZIPs regulate PIF4 beyond modulating its transcript levels, we overexpressed PIF4-HA under a 35S promoter in WT, *bzip17/60* and *bzip28/60* mutant backgrounds (Fig. 4a, b). Plants with comparable *PIF4* transcript levels were selected for further analysis (Fig. 4c). We found that PIF4-HA protein accumulation was impaired in *bzip* mutants as compared to WT under normal growth condition; nevertheless, the difference became more pronounced when plants were subjected to warmth treatment (Fig. 4d). Consistent with the reduced PIF4 levels, we also observed shorter hypocotyl lengths in *bzip* double mutant background as compared to WT.

To explore the roles of bZIPs in regulating PIF4 protein stability, we treated transgenic lines with cycloheximide (CHX) to block de novo protein synthesis and monitored PIF4 degradation over time. Upon CHX treatments, PIF4-HA degradation was accelerated in the *bzip28/60* mutants compared with WT under both normal and elevated

Fig. 3 | Activated bZIP transcription factors interact with PIF4 in the nucleus and bind PIF4-target promoters in a PIF4-dependent, temperature-responsive manner. a In vitro pull-down assays using MBP-tagged PIF4 incubated with mCherry, bZIP17N-mCherry, bZIP28N-mCherry, or bZIP60s-mCherry proteins. Interactions were detected via immunoblotting with anti-mCherry and anti-MBP antibodies. Red arrows indicate the target bands. The pull-down experiments were independently repeated three times with similar results. **b** Co-immunoprecipitation (Co-IP) assays using 10-day-old seedlings of overexpression lines (*UBQ::PIF4-flag/WT*, *35S::bZIP17N-HA/WT*, *35S::bZIP28N-HA/WT*, *UBQ::bZIP60s-flag/WT*, and their combinations). Seedlings were grown at 22 °C for 10 days and then either shifted to 29 °C or maintained at 22 °C for an additional 6 h. Extracts were immunoprecipitated with anti-flag magnetic beads, followed by immunoblotting for HA-tagged bZIP17N and bZIP28N (top panel) and myc-tagged PIF4 (bottom panel). Red asterisks indicate the target bands. The Co-IP experiments were independently repeated three times with similar results. **c** Bimolecular fluorescence complementation (BiFC) assays in *Nicotiana benthamiana* leaves co-transformed with PIF4-GFP^{C} and either GFP^{N}, GFP^{N}-bZIP17N, GFP^{N}-bZIP28N, or GFP^{N}–bZIP60s. Scale bar, 20 μm. The BiFC experiments were independently repeated three times with similar results. **d** Electrophoretic mobility shift assays (EMSA) showing the interaction of bZIP28N, bZIP17N and bZIP60s with PIF4 promoter probes containing G-box (CACGTG). DNA fragments of PIF4 upstream region containing a normal G-box motif and a mutated G-box motif (M-G-box, CAGGTG) were synthesized and labeled with biotin. Competitor is 100-fold unlabeled cold probe. MBP and mCherry protein were used as negative controls. The experiment was independently repeated three times with similar results. ChIP-qPCR analysis of **e** bZIP17N-HA, **f** bZIP28N-HA, and **g** bZIP60s-flag enrichment at promoter regions of PIF4 target genes (*PIF4*, *YUC8*, *IAA19*) under normal and warmth conditions. Chromatin from each sample was immunoprecipitated with anti-HA or anti-flag antibodies. Precipitated DNA was quantified by qPCR and analyzed using the percentage of input method. DNA enrichment is presented as the ratio between IP and mock (WT) control. *PP2A* served as an internal control. The error bars represent the s.d. (n = 3 biological replicates), and the centers of the error bars indicate the mean. Asterisks indicate significant difference (two-sided t-test; $^{*}P$-value < 0.05; $^{***}P$-value < 0.01).

temperatures (Fig. 4e, f). These results demonstrate that bZIPs are required to stabilize PIF4 protein in vivo. Moreover, the effect of bZIP28 and bZIP60 on PIF4 stability implicates these two major UPR regulators are collectively involved in thermomorphogenic signaling.

Additionally, we examined whether bZIPs influence PIF4 transcriptional activity. To ensure comparability, equivalent amount of PIF4-HA protein was used for ChIP assays. We found comparable binding of PIF4-HA to its target promoters (*pPIF4*, *pYUC8* and *pIAA19*) in both WT and *bzip* double mutants (Supplementary Fig. 10). These results suggest that the absence of bZIPs does not impair transcriptional activity of PIF4 but instead it reduces PIF4 protein stability thereby limiting its ability to promote hypocotyl elongation.

bZIP factors partially offsets phyB-mediated inhibition of PIF4 function

phyB is a red/far-red light photoreceptor that also functions as a thermosensor in Arabidopsis. At elevated temperatures, phyB undergoes thermal reversion to its inactive state, thereby releasing its suppression of PIF4 and enabling thermomorphogenic growth program[23,24].

To investigate the interplay between bZIPs and the PIF4-phyB module, we examined UPR activation in *phyB* mutant and *35S::YHB* plants, wherein the later expresses a constitutively active phyB variant (YHB, carrying a Y276H substitution) under warm condition. qPCR analysis suggested a wild-type level of *bZIP28* and *BiP1* expression in both backgrounds, indicating that phyB does not affect UPR activation under warm conditions (Supplementary Fig. 11).

We then assessed the impact of bZIP28 and bZIP60 on PIF4 stability in the context of phyB regulation. Thermomorphogenic responses were strongly suppressed in *35S::YHB* plants, whereas overexpression of bZIP28N or bZIP60s partially restored elongation at elevated temperature (Fig. 5a, b and Supplementary Fig. 12a). Consistently, increased PIF4 protein levels were detected in *bZIP28N/35S::YHB* and *bZIP60s/35S::YHB* seedlings compared with *35S::YHB* alone, and the repression of *YUC8* by YHB was alleviated in these lines (Supplementary Fig. 12b, c). These results together demonstrate that bZIP28N and bZIP60s counteract the inhibitory effect of phyB on PIF4 accumulation and function under warm condition.

Pull-down and BiFC assays showed that bZIP17N, bZIP28N, and bZIP60s directly interact with phyB in vitro and in vivo (Fig. 5c, d). To test whether bZIPs affect the phyB-PIF4 interaction in planta, we performed firefly luciferase complementation imaging (LCI) assays in Nicotiana. Co-expression of PIF4-cLuc and phyB-nLuc generated a robust luciferase signal, confirming their in vivo interactions. Notably, co-expression of bZIP28N-YFP or bZIP60s-YFP strongly reduced the PIF4-phyB interaction (Fig. 5e, f). These findings indicate that the major UPR regulators bZIP28N and bZIP60s stabilize PIF4 by competitively attenuating its interaction with phyB, thereby promoting PIF4 function under warm conditions.

Previous work showed that HSFA1s stabilize PIF4 during thermomorphogenesis without affecting its DNA-binding capacity[25]. Given that UPR-associated bZIPs also stabilize PIF4, we asked whether these pathways might intersect. Pull-down assays revealed that bZIPs directly interact with HSFA1d, but such interactions are independent of PIF4 (Supplementary Fig. 13a). Moreover, in the *hsfa1* quadruple mutant, bZIPs still interact with PIF4, indicating that their association is HSFA1-independent (Supplementary Fig. 13b). We further interrogated published RNA-seq data of short-term warm-treatment and found that transcripts of *HSFA1* accumulate later than those of *bZIP28* and *PIF4*[18]. Together, these observations imply that bZIPs and HSFA1s may act on the regulation of PIF4 stability in a sequential order, wherein bZIPs contribute to early stabilization of PIF4, which is further reinforced by HFSA1s during prolonged warming possibly in a joint effort with bZIPs. Future studies are therefore required to dissect the underlying molecular mechanism in detail.

Discussion

Plants integrate environmental cues with developmental programs to optimize growth under fluctuating temperatures[26–28]. Thermomorphogenesis, characterized by hypocotyl elongation and other morphological adjustments, is primarily regulated by PIF4[26]. Whereas PIF4-mediated temperature responses have been well studied, the contribution of cellular stress pathways, particularly the UPR, to thermomorphogenic growth remain unclear.

Here, we show that the UPR-associated transcription factors bZIP17, bZIP28, and bZIP60 promote thermomorphogenesis by stabilizing PIF4 protein and facilitating the expression of growth-related genes (Figs. 2 and 4). Warm temperatures rapidly activate UPR signaling, as indicated by early accumulation of *bZIP28* and *BiP1* transcripts, proceeding PIF4 induction (Fig. 1). The active bZIPs translocate to the nucleus and interact with PIF4, forming complexes that bind to promoters of PIF4 target genes, including *PIF4* itself and *YUC8*, thereby promoting thermomorphogenic growth (Fig. 3). These effects are strictly PIF4-dependent, as bZIP overexpression fails to rescue the thermomorphogenic defect in the *pif4* mutant (Fig. 2). Consistently, ChIP-qPCR analysis confirmed that bZIPs binding to these promoters depend on PIF4, reinforcing the central role of PIF4 in regulating thermomorphogenesis. Our findings support direct promoter binding by active bZIPs, while leaving open the possibility that PIF4 may additionally facilitate bZIP recruitment by enhancing chromatin accessibility.

The dominant roles of bZIP28 and bZIP60 in thermomorphogenesis are consistent with their primary functions in the canonical UPR pathway, whereas bZIP17 contributes more modestly.

https://doi.org/10.1038/s41467-025-67909-9

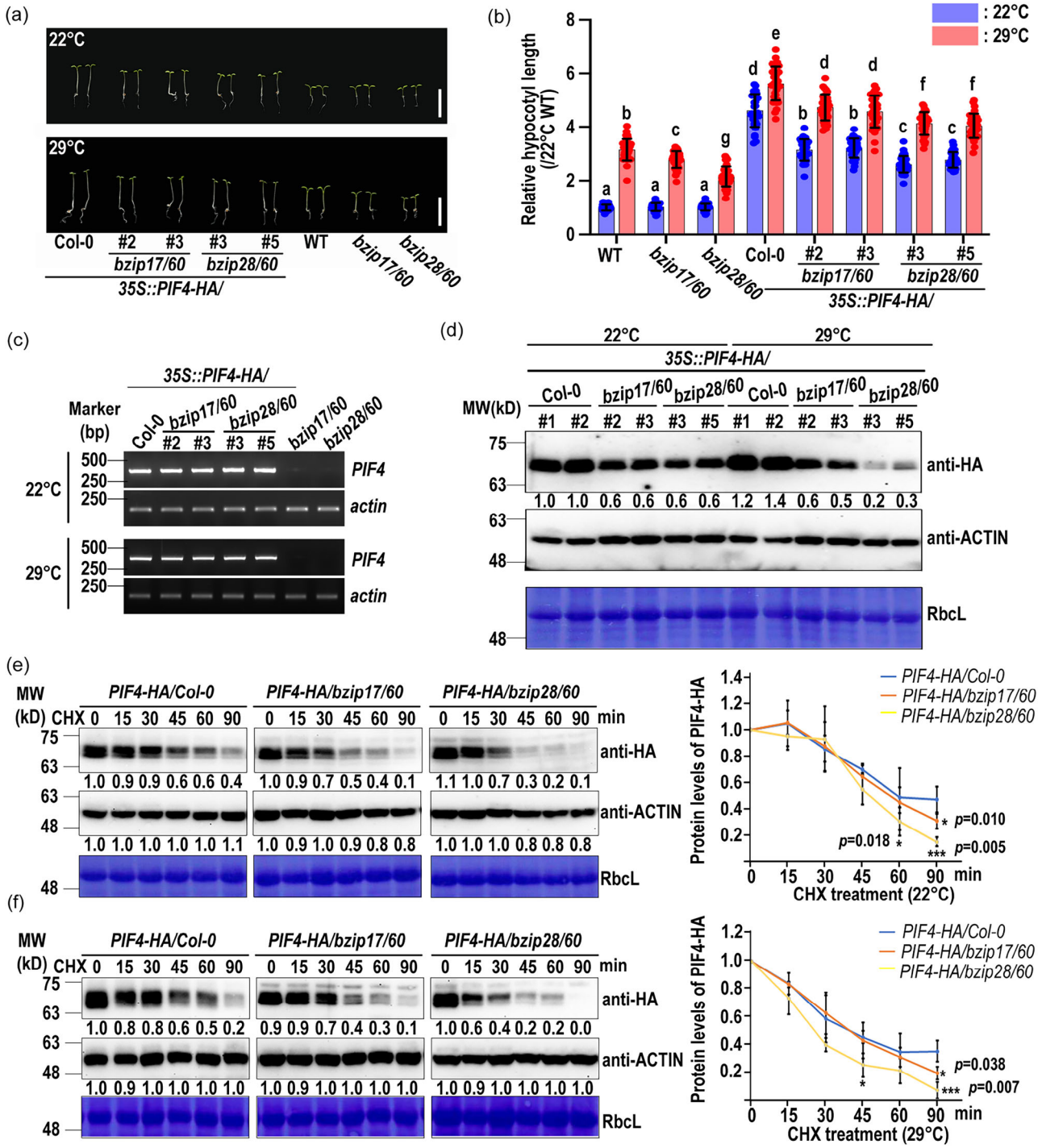

Fig. 4 | bZIP transcription factors promote PIF4 protein accumulation. **a** Representative images of 5-day-old seedlings of the indicated genotypes (WT, *bzip17/60*, and *bzip28/60*, *35S::PIF4-HA/WT*, 2 independent *35S::PIF4-HA/bzip17/60* lines (#2 and #3), and 2 independent *35S::PIF4-HA/bzip28/60* lines (#3 and #5)) grown at 22 °C or 29 °C. Scale bar, 1 cm. **b** Hypocotyl length measurements of the seedlings shown in (**a**), normalized to WT at 22 °C (1.6 mm). The error bars represent the s.d. (n = 33 biological replicates), and the centers of the error bars indicate the mean. Different lowercase letters represent statistically significant differences (one-way ANOVA, Tukey's test, $P < 0.05$). **c** Semi-quantitative RT-PCR analysis of PIF4-HA mRNA levels in the same lines as in (**a**). *actin* transcription levels were used as a control. **d** Immunoblot analysis showing PIF4-HA levels in seedlings of various genotypes. ACTIN and RbcL levels were used as loading controls. Band intensity in the WT sample (target band intensity/ ACTIN intensity) at 22 °C was set to 1 and the relative values were quantified by ImageJ. The experiment was independently repeated three times with similar results. Time-course analysis of PIF4-HA protein stability following cycloheximide (CHX) treatment at 22 °C (**e**) or 29 °C (**f**). Left panel: Representative immunoblots showing PIF4-HA protein levels at different time points after CHX treatment. ACTIN and RbcL levels served as loading controls. Right panel: Quantification of PIF4 degradation. Protein levels are shown relative to the WT-0h time point (set as 1). The error bars represent the s.d. (n = 3 biological replicates), and the centers of the error bars indicate the mean. Asterisks indicate significant difference (two-sided t-test; $^{*}P$-value < 0.05; $^{***}P$-value < 0.01).

https://doi.org/10.1038/s41467-025-67909-9

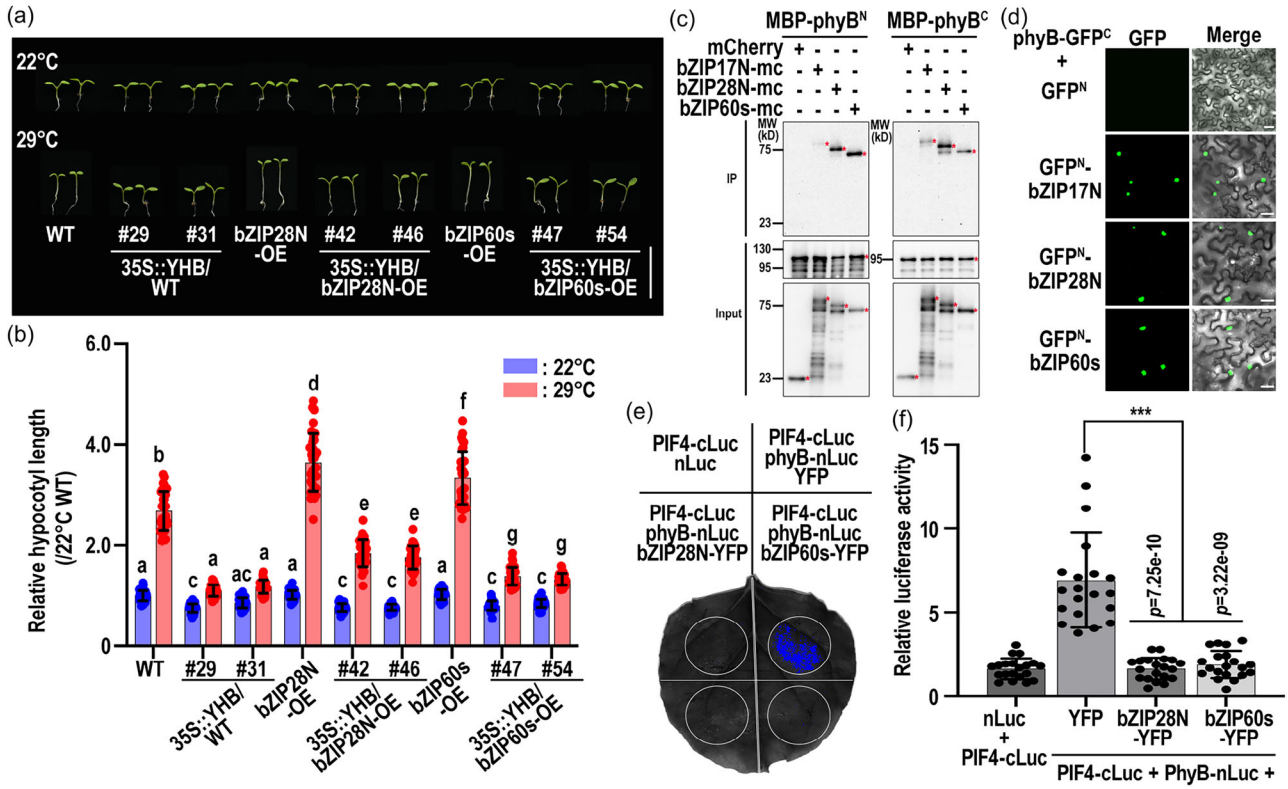

Fig. 5 | bZIP transcription factors compete with phyB for PIF4 binding to counteract phyB-mediated inhibition. a Representative images of 5-day-old seedlings of the indicated genotypes (WT, bZIP28N-OE, bZIP60s-OE, 2 independent *35S::YHB/WT* lines, 2 independent *35S::YHB/bZIP28N-OE* lines and 2 independent *35S::YHB/bZIP60s-OE* lines) grown at 22 °C or 29 °C. Scale bar, 1 cm. **b** Hypocotyl length measurements of the seedlings shown in (**a**), normalized to WT at 22 °C (1.6 mm). The error bars represent the s.d. (n = 33 biological replicates), and the centers of the error bars indicate the mean. Different lowercase letters represent statistically significant differences (one-way ANOVA, Tukey's test, $P < 0.05$). **c** In vitro pull-down assays using MBP-tagged N-terminal phyB (phyB^N) or C-terminal phyB (phyB^C) incubated with mCherry, bZIP17N-mCherry, bZIP28N-mCherry, or bZIP60s-mCherry proteins. Interactions were detected via immunoblotting with anti-mCherry and anti-MBP antibodies. Red asterisks indicate the target bands. The experiment was independently repeated three times with similar results. **d** Bimolecular fluorescence complementation (BiFC) assays in Nicotiana leaves co-transformed with phyB-GFP^C and either GFP^N, GFP^N-bZIP17N, GFP^N-bZIP28N, or GFP^N–bZIP60s. Scale bar, 20 μm. The experiment was independently repeated three times with similar results. **e** Firefly luciferase (LUC) complementation imaging (LCI) assays showing that bZIP28N and bZIP60s inhibit PIF4/phyB interaction in vivo. Nicotiana leaves were co-transformed with the constructs as indicated in the top panel. **f** Relative luciferase activity shown in (**e**). The error bars represent the s.d. (n = 22 biological replicates), and the centers of the error bars indicate the mean. Unpaired two-sided t-test; $^{***}P < 0.01$.

Arabidopsis seedlings overexpressing bZIP28N exhibit longer hypocotyls under warm conditions (Fig. 2e and Supplementary Fig. 6). Hypocotyl elongation in bZIP60s-OE lines is slightly less pronounced than in bZIP28N-OE, likely due to relatively lower expression levels (Fig. 2e and Supplementary Fig. 6). Additionally, *bzip28/60* double mutants display shorter hypocotyls than *bzip17/60* mutants (Fig. 2a). Consistently, PIF4 stability assays indicate that bZIP28 and bZIP60 are more critical for promoting thermomorphogenic growth, highlighting their dominant roles (Fig. 4e, f). The combinational mutation of three UPR-modulatory bZIPs leads to seedling lethality. This hindered us from systemically dissecting the role of all 3 bZIPs in regulating thermomorphogenesis, especially given that *pif4* is completely insensitive to warmth treatment whereas minor hypocotyl elongation could still be observed in *bZIP* double knockout mutants. Moreover, single mutant *bzip17*, *bzip28*, or *bzip60* show no detectable hypocotyl defects under warm conditions, consistent with their minimal growth defects in response to Tm, indicative of functional redundancy[29,30] (Fig. 2a).

Given the central role in thermomorphogenic responses, PIF4 function is tightly regulated by phyB photoreceptor. Our data suggest that bZIP28N and bZIP60s antagonize phyB-mediated PIF4 degradation. In seedlings expressing constitutively active phyB (35S::YHB), overexpression of bZIP28N or bZIP60s partially restored PIF4 accumulation and hypocotyl elongation (Fig. 5a). LCI assay indicated that bZIPs interfere with the PIF4-phyB interaction, thereby promoting PIF4 accumulation under warm conditions (Fig. 5e, f). The bZIP-PIF4 association remains stable at both 22 °C and 29 °C (Supplementary Fig. 8), suggesting that the complex is maintained once formed. Future studies are thus required to capture its dynamics during early activation. Intriguingly, pervious work has shown that phyB promotes UPR signaling under red light[31]. It is therefore likely that phyB has more general functions in regulating UPR signaling, which serves as an interesting avenue for future investigation.

Based on our findings, we proposed a working model illustrating how UPR-associated bZIPs integrate with the phyB-PIF4 module to regulate thermomorphogenesis (Fig. 6). Warm temperatures induce ER stress, triggering the activation and nuclear translocation of bZIP17, bZIP28, and bZIP60. In the nucleus, these bZIPs interact with PIF4 and simultaneously associate with active phyB, reducing phyB-mediated PIF4 turnover. This stabilizes PIF4 protein, enabling activation of growth-promoting genes and driving adaptive hypocotyl elongation.

In summary, our study established a previously unrecognized link between UPR signaling and plant growth regulation under elevated temperature. By connecting ER stress responses with thermomorphogenesis, we reveal how plants coordinate environmental stress adaptation with developmental plasticity. Given the central role of the UPR in diverse stress responses, UPR-associated bZIPs may broadly influence other stress-related adaptive growth pathways, providing

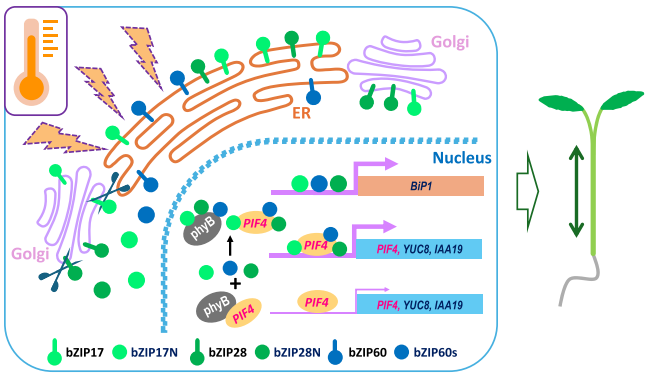

Fig. 6 | Model of UPR-PIF4-phyB crosstalk in thermomorphogenesis. Elevated temperature activates the UPR leading to the proteolytic processing of bZIP17 and bZIP28 and their subsequent nuclear translocation. In parallel, bZIP60 transcripts undergo splicing, producing a nuclear-localized bZIP60 isoform. These activated bZIP transcription factors induce *BiP1* expression to relieve ER stress. Moreover, they also physically associate with PIF4, enabling bZIP-PIF4 complexes to bind and activate PIF4 target gene promoters. In addition, bZIPs interact directly with phyB and attenuate the phyB-PIF4 association, thereby stabilizing PIF4 and enhancing hypocotyl elongation under warm conditions.

new insight into how plants integrate environmental signals to optimize growth and survival under climate-induced stress.

Methods

Plant materials and construction of transgenic plants

Wild-type (WT) and mutant plants of *Arabidopsis thaliana* (hereafter Arabidopsis; Columbia-0, Col-0 ecotype) were used in this study. The T-DNA insertion mutants *bzip17* (SALK_104326), *bzip28* (SALK_132285C), *bzip60* (SALK_050203), and *pif4* (CS66043) were obtained from the Arabidopsis Biological Resource Center (ABRC). Double mutants *bzip17/60* and *bzip28/60* were obtained from Prof. Jeanmarie Verchot[32]. Triple mutants *bzip17/60/pif4* and *bzip28/60/pif4* were generated by genetic crosses. The *hsfa1-cq* mutant was obtained from Prof. Wenqiang Tang's laboratory.

To generate full-length *bZIP17*, *bZIP28* and *bZIP60* overexpression lines in the WT background, the coding sequences of these genes were cloned into pBA-GFP^{N}-DC vector via the Gateway system to produce 35S::*GFP^{N}-bZIPs*.

For overexpression of the N-terminal fragments *bZIP17N* and *bZIP28N* in WT background, DNA sequences encoding the N-terminal fragment of bZIP17 (amino acids 1 to 366, 1098 bp) and bZIP28 (amino acid 1 to 323, 969 bp) were cloned into pBA-DC-HA vector using the Gateway system (Invitrogen, US). The resulting constructs were 35S::*bZIP17N-HA* (bZIP17N-OE) and 35S::*bZIP28N-HA* (bZIP28N-OE), respectively. For *bZIP60s* overexpression in WT, DNA sequences encoding the spliced form of *bZIP60* were synthesized by Bio Basic Company (Canada) and cloned into the pUBQ-DC-flag vector to generate UBQ::*bZIP60s-flag* (bZIP60s-OE).

These constructs were used to generate transgenic bZIPs-OE lines, which were then crossed with the *pif4* mutant to obtain bZIPs-OE/*pif4* seedlings.

For *PIF4* overexpression in the WT, *bzip17/60*, or *bzip28/60* double mutant, the full-length *PIF4* coding sequence was cloned into pUBQ-DC-flag, pBA-DC-myc or pBCO-DC-HA vectors to generate UBQ::*PIF4-flag*, 35S::*PIF4-myc* or 35S::*PIF4-HA*, respectively. These constructs were introduced into Arabidopsis through *Agrobacterium tumefaciens* (GV3101)-mediated floral dipping transformation[33]. Double transgenic plants, including *bZIP17N-HA/PIF4-myc*, *bZIP28N-HA/PIF4-myc*, *bZIP17N-HA/PIF4-flag*, *bZIP28N-HA/PIF4-flag* and *bZIP60s-flag/PIF4-myc*, *bZIP17N/60s-OE*, *bZIP28N/60s-OE* in both WT and *pif4* background, were obtained by genetic crosses.

For *YHB* overexpression in the WT, bZIP28N-OE, and bZIP60s-OE seedlings, the full-length phyB coding sequence was first cloned into pENTY vector. A site-directed mutation (Y276H substitution) was then introduced to generate YHB, which was subsequently cloned into pBA-DC-myc vector to generate 35S::*YHB-myc*.

Plant growth conditions and treatments

Arabidopsis and *Nicotiana benthamiana* (hereafter Nicotiana) plants were grown in a greenhouse at 22 °C under long-day conditions (16-h light/8-h dark). Seeds were surface sterilized for 10 min in 70% (v/v) ethanol, followed by a wash in 98% (v/v) ethanol and let dry on a sterile bench. Seeds were sown on half-strength Murashige and Skoog (MS) media solidified with 0.8% agar (w/v) and supplemented with 1% sucrose (w/v). The seeds were stratified at 4 °C for 2 days in the dark and then transferred to a chamber with LED light illumination (70 μmol $m^{-2}s^{-1}$) under 16 h light/8 h dark.

For the time course experiment at 29 °C, seedlings were grown at 22 °C for 3 days before being transferred to 29 °C or kept at 22 °C for 10, 20, 30, 40, 50, 60, 120, 180, 240 min, 5 h, 1, 2, 3, 4, 5, 6, 7, 9, 11, and 13 additional days. Samples taken at the indicated time point were frozen in liquid nitrogen.

For hypocotyl elongation measurements, mutant seedlings were grown on plates at 22 °C for 3 days and then transferred to 29 °C or kept at 22 °C for 4 additional days. Overexpression seedlings were grown at 22 °C for 2 days and transferred to 29 °C or kept at 22 °C for 3 additional days. After the treatment period, images of seedlings were taken and hypocotyl lengths were measured using ImageJ software.

Seedling grown at 22 °C for 7 days were used for analysis of transcript and protein levels. Seedlings were either maintained at 22 °C or transferred to 29 °C for an additional 6 h (for mutant seedlings) or 3 h (for overexpression seedlings). Samples were frozen in liquid nitrogen.

RNA expression analysis

Total RNAs were extracted using EasyPure Plant RNA Kit (Transgen, China). Reverse transcription (RT) was performed using 1 μg RNA and PrimeScript™ RT Master Mix (Takara, Japan) following the manufacturer's instructions. The cDNA solution was diluted (1:2) with nuclease-free water. Quantitative PCR (qPCR) was performed using SYBR Green Master (Bio-Rad, USA) on Bio-Rad CFX96 real-time system. Expression levels of target genes were normalized by *actin* transcript levels. Semi-quantitative PCR were performed using specific primers to detect transgenic *PIF4* cassette. All primers are listed in Supplementary Table 1. All experiments were performed with at least three independent biological replicates.

Immunoblotting

Seedlings were homogenized in liquid nitrogen, and lithium dodecyl sulfate (LDS) buffer was added at a ratio of 1:3 (fresh weight: buffer). Protein samples were boiled for 10 min and separated on 10% SDS-PAGE gels. Gels were transferred to 0.45 μm PVDF membranes (Merck, USA), followed by incubation in blocking buffer (1X TBS buffer including 0.1% Tween 20 and 5% dried nonfat milk) for 1 h at room temperature. Membranes were then incubated overnight at 4 °C with anti-PIF4 (Agrisera, Cat no. AS163955; 1:3000), anti-myc (Santa Cruz, sc-40; 1:3000), anti-HA (Santa Cruz, sc-7392X; 1:3000) or anti-ACTIN (Proteintech, 60008-1-Ig; 1:5000). Afterward, membranes were incubated for 1 h with a peroxidase-conjugated secondary antibody: anti-mouse (cytiva, NXA931; 1:5000), anti-rabbit (cytiva, NA934; 1:5000) or anti-Goat (Agrisera, AS09605: 1:2000). ACTIN levels, measured by Western blots and the Coomassie blue stained gel band of RbcL (RUBISCO large subunit) were used as loading controls. Fluorescent signals were captured on iBright (Invitrogen, USA).

Protein expression and purification

The coding sequences of *bZIP17N*, *bZIP28N*, and *bZIP60s* were cloned into pET28a-mCherry to generate *His-bZIP-mCherry* constructs. The CDS of *PIF4* was cloned into pET28a to generate His-PIF4 construct. The CDS of HSFA1d, N-, or C-terminal of phyB, *PIF4* was cloned into pMAL-DC vector to generate *MBP-HSFA1d, MBP-phyB^N, MBP-phyB^C, and MBP-PIF4* construct, respectively. Protein expression constructs were transformed into *Escherichia coli* strain Rosetta (Novagen/Merck, Darmstadt, Germany), and recombinant proteins were expressed and purified as described previously[34]. Briefly, induced cells were suspended in lysis buffer (50 mM Tris-HCl pH 7.4, 200 mM NaCl, 1 mM $MgCl_2$, 1 mg/ml lysozyme, 10% Glycerol) and gently shaken for 30 min in a cold room. Bacterial cells were lysed by sonication (Qsonica, Newtown, CT, USA) on ice at 40% amplitude, 15 s on/30 s off, 15 cycles, and TritonX-100 was then added to a final concentration of 1%. Cell lysates were centrifuged at 21,000 × *g* for 1 h (Beckman Coulter, Pasadena, CA, USA). The supernatant was mixed with equilibrated amylose (NEB, Ipswich, MA, USA) or Ni-NTA (Bio Basic Inc. Canada) beads, and protein purification was carried out according to the manufacturers' instructions. Protein purity was assessed by SDS-PAGE.

In vitro pull-down assays

500 ng of purified proteins were incubated in reaction buffer (20 mM Tris-HCl pH7.4, 150 mM NaCl, 0.2% glycerol, and protease inhibitor (Roche)) for 1 h at room temperature (RT). Equilibrated resins were added to the mixture, which was then further incubated for 1 h at RT. The resins with bound proteins were washed 5 times with the reaction buffer. Bound proteins were eluted by LDS and incubated at 98 °C for 5 min. Proteins in samples were separated by SDS-PAGE followed by Western blot analysis using anti-MBP (Proteintech, Cat no. 66003-1-Ig; 1:3000) and anti-mCherry (Proteintech, Cat no. 26765-1-AP; 1:3000).

Electrophoretic mobility shift assay (EMSA)

EMSA were performed using Biotin 3' End DNA Labeling Kit and Lightshift Chemiluminescent EMSA kit according to the manufacturer's instructions (Thermo Scientific). MBP, MBP-bZIP28N, -bZIP17N, mCherry, mCherry-bZIP60s recombinant proteins were incubated in a 20 µl reaction mixture containing 100 mM Tris-HCl pH8.0, 50 mM KCl, 5 mM $MgCl_2$, 0.05% NP-40, 1 mM EDTA, 50 ng/ml poly (dI-dC) for 10 min at room temperature. The biotin-labeled probes were then added to the mixture and incubated for additional 20 min at room temperature before separation on 4% native polyacrylamide gels in 0.5X TBE buffer. The labeled probes were detected with streptavidin according to the instructions provided by the manufacturer (Pierce).

Chromatin immunoprecipitation (ChIP) assays

ChIP experiments were performed as described previously[35]. Ten-day-old WT, *bZIP17N-OE/WT*, *bZIP17N-OE/pif4*, *bZIP28N-OE/WT*, *bZIP28N-OE/pif4*, *bZIP60s-OE/WT* and *bZIP60s-OE/pif4* seedlings, transferred to 29 °C for 5 h or kept at 22 °C, were used for ChIP assays. Approximately 2 g of each sample was harvested and cross-linked in 1% formaldehyde for 15 min, followed by 5-min neutralization with 0.125 M glycine. After washing 6 times with distilled water, seedlings were ground into powder in liquid nitrogen. Chromatin complexes were isolated and sonicated. The specific chromatin complex was then immunoprecipitated using anti-HA (Santa Cruz Antibodies, Cat no. sc-7392 X; 1:3000) or anti-flag antibody (lab-made). The precipitated DNA was recovered and analyzed by real-time qPCR using the respective primer pairs listed in Supplementary Table 1.

Agrobacterium-mediated transient overexpression

For the co-localization experiment, the coding sequences of *bZIP17N, bZIP28N and bZIP60s* were cloned into pBA-DC-GFP, and *YHB* or *PIF4* was cloned into pBA-DC-CFP. For the BiFC assay, the coding sequences of *bZIP17N, bZIP28N and bZIP60s* were cloned into the pBA-GFP^N-DC, and *PIF4* was cloned into pBA-DC-GFP^C using Gateway system.

These binary vectors were transformed into Agrobacterial GV3101, and colony was inoculated into liquid LB medium and grown overnight. Harvested cells were resuspended in the Agrobacterium resuspension buffer (10 mM $MgCl_2$, 10 mM MES and 0.2 mM acetosyringone) to an optical density of ~1.0 at 600 nm (OD600) and allowed to sit for 2–3 h. Nicotiana leaves were then infiltrated with the bacterial suspension using a 1-mL syringe without a needle. Leaves were examined for fluorescence signal at 2 days post agroinfiltration by Confocal microscopy (FV3000 confocal laser scanning microscope, Olympus, Japan). Excitation wavelengths used were 488 nm for GFP and 406 nm for CFP. Pearson's correlation coefficient (PCC) was calculated using CellSens software based on confocal images acquired with the FV3000 microscope.

Co-immunoprecipitation assays

Transgenic plants expressing bZIP17N, bZIP28N, bZIP60s, PIF4 or their combinations were used to detect possible interactions. Seedlings were grown in a chamber at 22 °C under long-day conditions for 7 days before being transferred to 29 °C for 5 h. Harvested samples were ground into a fine powder in liquid nitrogen and homogenized in 2X IP buffer (50 mM Tris-HCl, pH 7.5, 150 mM NaCl, 1 mM EDTA, 0.5% Triton X-100, 5% Glycerol, 50 µM MG132, protease inhibitor cocktail tablets (Roche)). Extracts were centrifuged two times at 12,000 × *g* for 20 min. The supernatant was mixed with 40 µl anti-myc magnetic beads (for bZIP28N and PIF4 interaction test) (Santa Cruz, sc-500772) or anti-flag M2 magnetic beads (Merck, Cat no. M8823) for 4 h at 4°. The beads were then washed 5 times with 1X IP buffer. Samples were boiled in SDS-PAGE sample buffer, and the co-immunoprecipitated proteins were detected with anti-HA, anti-flag or anti-myc antibody (Cell Signaling Technology, Cat no. #2276; 1:3000).

ER stress treatment and phenotypic analysis

Experiments with Tunicamycin (Tm) were performed by growing seedlings directly on plates containing various concentrations (8, 40, 60 and 80 µg/L) of Tm (Sigma-Aldrich, Cat no. T7765). Tm was replaced by the same volume of dimethyl sulfoxide (DMSO) in control treatment. After 3 days at 22 °C, seedlings on 8 µg/L Tm or DMSO plates were transferred to 29 °C or kept at 22 °C for 4 additional days. Seedlings images were captured and hypocotyl lengths were measured by ImagJ. For normal phenotypic analysis of ER stress, shoot (grown horizontally) and primary root growth (grown vertically) of 7d-old seedlings were captured. Root lengths were measured by ImageJ software. For qRT-PCR analyzes, seedlings were grown on half MS medium with 1% sucrose and 0.8% agar for 10 days, followed by transfer to 5 µg/ml Tm plates for 5 h. All data shown are the mean of at least 3 independent biological experiments.

Protein degradation assessments

10-day-old seedlings of *PIF4-HA/WT*, *PIF4-HA/bzip17/60* and *PIF4-HA/bzip28/60* were transferred to MS liquid medium and incubated overnight. To examine the half-life of PIF4-HA proteins in these genotypes, seedlings were treated with 50 µM MG132 for 6 h to block proteasome activity. After washing three times, seedlings were transferred to a medium containing 200 µM cycloheximide (Sigma-Aldrich, Cat no. C1988) to stop new protein synthesis. Samples were harvested at different time points, and protein extracts were analyzed by immunoblotting.

Firefly LCI assays

The LCI assays for the protein interaction detection were performed in *N.benthamiana* leaves as described previously[36–38]. Briefly, the full-length of the genes was cloned into pCAMBIA1300-nLuc or pCAMBIA1300-cLuc vectors, respectively. These vector constructs and

control vectors were transformed into *Agrobacterium* strain GV3101. The bacteria that contain nLuc or cLuc constructs were cultured overnight and then mixed in equal ratios. The bacterial mixtures were then introduced into *N.benthamiana* leaves using a needle-less syringe. Before imaging, the leaves were infiltrated with 1 mM D-luciferin and then kept in the dark for 5 min. The LUC activities were analyzed after 48-h infiltration using Retiga LUMO CCD (Teledyne, Canada).

Accession numbers

For Arabidopsis genes, accession numbers given by the Arabidopsis Information Resource (https://www.arabidopsis.org/) are indicated. *bZIP17* (*AT2G40950*), *bZIP28* (*AT3G10800*), *bZIP60* (*AT1G42990*), *PIF4* (*AT2G43010*), *actin* (*AT3G18780*), *BiP1* (*AT5G28540*), *BiP3* (*AT1G09080*), *YUC8* (*AT4G28720*), *IAA19* (*AT3G15540*), *PP2A* (*AT1G69960*), phyB (*AT2G18790*), *HSFA1d* (*AT1G32330*).

Statistical analyses

Data are presented as mean ± standard deviation, with error bars indicating the standard deviation. Comparisons between two groups were performed using a two-tailed Student's *t*-test in Microsoft Excel 2016. $P < 0.05$ considered statistically significant, and $P < 0.01$ highly significant. Comparisons among more than two groups were conducted using one-way ANOVA followed by Tukey's post hoc test, performing using the Statistics Kingdom online tool.

Reporting summary

Further information on research design is available in the Nature Portfolio Reporting Summary linked to this article.

Data availability

Arabidopsis genotypes used in the current study are available from the corresponding author upon request. Source data are provided with this paper.

References

1. Cramer, G. R., Urano, K., Delrot, S., Pezzotti, M. & Shinozaki, K. Effects of abiotic stress on plants: a systems biology perspective. *BMC Plant Biol.* **11**, 163 (2011).
2. Gray, S. B. & Brady, S. M. Plant developmental responses to climate change. *Dev. Biol.* **419**, 64–77 (2016).
3. Georgieva, M. & Vassileva, V. Stress management in plants: examining provisional and unique dose-dependent responses. *Int. J. Mol. Sci.* **24**, 5105 (2023).
4. Manghwar, H. & Li, J. Endoplasmic reticulum stress and unfolded protein response signaling in plants. *Int. J. Mol. Sci.* **23**, 828 (2022).
5. Liu, Y. et al. Unfolded protein response in balancing plant growth and stress tolerance. *Front. Plant Sci.* **13**, 1019414 (2022).
6. Howell, S. H. Endoplasmic reticulum stress responses in plants. *Annu. Rev. Plant Biol.* **64**, 477–499 (2013).
7. Ko, D. K. & Brandizzi, F. Dynamics of ER stress-induced gene regulation in plants. *Nat. Rev. Genet.* **25**, 513–525 (2024).
8. Gao, H., Brandizzi, F., Benning, C. & Larkin, R. M. A membrane-tethered transcription factor defines a branch of the heat stress response in *Arabidopsis thaliana*. *Proc. Natl. Acad. Sci. USA* **105**, 16398–16403 (2008).
9. Deng, Y. et al. Heat induces the splicing by IRE1 of a mRNA encoding a transcription factor involved in the unfolded protein response in *Arabidopsis*. *Proc. Natl. Acad. Sci. USA.* **108**, 7247–7252 (2011).
10. Deng, Y. et al. IRE1, a component of the unfolded protein response signaling pathway, protects pollen development in *Arabidopsis* from heat stress. *Plant J.* **88**, 193–204 (2016).
11. Zhang, S. S. et al. Tissue-specific transcriptomics reveals an important role of the unfolded protein response in maintaining fertility upon heat stress in *Arabidopsis*. *Plant Cell* **29**, 1007–1023 (2017).
12. Gao, J., Wang, M. J., Wang, J. J., Lu, H. P. & Liu, J. X. bZIP17 regulates heat stress tolerance at reproductive stage in *Arabidopsis*. *aBIOTECH* **3**, 1–11 (2021).
13. Sun, Y. et al. VvFHY3 links auxin and endoplasmic reticulum stress to regulate grape anthocyanin biosynthesis at high temperatures. *Plant Cell* **37**, koae303 (2024).
14. Bajaj, M., Allu, A. D. & Rao, B. J. Dynamic regulation of protein homeostasis underlies acquired thermotolerance in *Arabidopsis thaliana*. Preprint at *bioRxiv* https://www.biorxiv.org/content/10.1101/2023.08.04.552042v2 (2023).
15. Quint, M. et al. Molecular and genetic control of plant thermomorphogenesis. *Nat. Plants* **2**, 15190 (2016).
16. Casal, J. J. & Balasubramanian, S. Thermomorphogenesis. *Annu. Rev. Plant Biol.* **70**, 321–346 (2019).
17. Delker, C., Quint, M. & Wigge, P. A. Recent advances in understanding thermomorphogenesis signaling. *Curr. Opin. Plant Biol.* **68**, 102231 (2022).
18. Li, B. et al. Heat Shock Factor A1s are required for phytochrome-interacting factor 4-mediated thermomorphogenesis in Arabidopsis. *J. Integr. Plant Biol.* **66**, 20–35 (2024).
19. Chen, D. et al. Antagonistic basic helix-loop-helix/bZIP transcription factors form transcriptional modules that integrate light and reactive oxygen species signaling in *Arabidopsis*. *Plant Cell* **25**, 1657–1673 (2013).
20. Ribeiro, B. et al. Interference between ER stress-related bZIP-type and jasmonate-inducible bHLH-type transcription factors in the regulation of triterpene saponin biosynthesis in *Medicago truncatula*. *Front. Plant Sci.* **13**, 903793 (2022).
21. Xu, Y. & Zhu, Z. PIF4 and PIF4-interacting proteins: at the nexus of plant light, temperature and hormone signal integrations. *Int. J. Mol. Sci.* **22**, 10304 (2021).
22. Ezer, D. et al. The G-Box transcriptional regulatory code in *Arabidopsis*. *Plant Physiol.* **175**, 628–640 (2017).
23. Jung, J. H. et al. Phytochromes function as thermosensors in *Arabidopsis*. *Science* **354**, 886–889 (2016).
24. Kim, S. et al. The epidermis coordinates thermoresponsive growth through the phyB-PIF4-auxin pathway. *Nat. Commun.* **11**, 1053 (2020).
25. Tan, W. et al. The heat response regulators HSFA1s promote *Arabidopsis* thermomorphogenesis via stabilizing PIF4 during the day. *Sci. Adv.* **9**, eadh1738 (2023).
26. Casal, J. J. & Qüesta, J. I. Light and temperature cues: multitasking receptors and transcriptional integrators. *New Phytol.* **217**, 1029–1034 (2018).
27. Li, X., Liang, T. & Liu, H. How plants coordinate their development in response to light and temperature signals. *Plant Cell* **34**, 955–966 (2022).
28. Song, J. et al. Florigen and florigen-Like genes regulate temperature-responsive flowering in tomato. *Adv. Sci.* **12**, e06711 (2025).
29. Kim, J. S., Yamaguchi-Shinozaki, K. & Shinozaki, K. ER-anchored transcription factors bZIP17 and bZIP28 regulate root elongation. *Plant Physiol.* **176**, 2221–2230 (2018).
30. Kim, J. S. et al. *Arabidopsis* TBP-ASSOCIATED FACTOR 12 ortholog NOBIRO6 controls root elongation with unfolded protein response cofactor activity. *Proc. Natl. Acad. Sci. USA* **119**, e2120219119 (2022).
31. Ahn, G. et al. Phytochrome B positively regulates red light-mediated ER stress response in *Arabidopsis*. *Front. Plant Sci.* **13**, 846294 (2022).
32. Gayral, M. et al. Multiple ER-to-nucleus stress signaling pathways are activated during Plantago asiatica mosaic virus and Turnip mosaic virus infection in *Arabidopsis thaliana*. *Plant J.* **103**, 1233–1245 (2020).
33. Clough, S. J. & Bent, A. F. Floral dip: a simplified method for Agrobacterium-mediated transformation of Arabidopsis thaliana. *Plant J.* **16**, 735–743 (1998).

34. Park, S.-H. et al. Arabidopsis ubiquitin-specific proteases UBP12 and UBP13 shape ORE1 levels during leaf senescence induced by nitrogen deficiency. *New Phytol.* **223**, 1447–1460 (2019).
35. Gendrel, A.-V., Lippman, Z., Martienssen, R. & Colot, V. Profiling histone modification patterns in plants using genomic tiling microarrays. *Nat. Methods* **2**, 213–218 (2005).
36. Sun, J. et al. PIF4 and PIF5 transcription factors link blue light and auxin to regulate the phototropic response in *Arabidopsis*. *Plant Cell* **25**, 2102–2114 (2013).
37. Dong, H. et al. Photoexcited phytochrome B interacts with brassinazole resistant 1 to repress brassinosteroid signaling in *Arabidopsis*. *J. Integr. Plant Biol.* **62**, 652–667 (2020).
38. Yang, Z. et al. BIC1 acts as a transcriptional coactivator to promote brassinosteroid signaling and plant growth. *EMBO J.* **40**, e104615 (2021).

Acknowledgements

We thank Prof. Jeanmarie Verchot (TEXAS A&M UNIVERSITY, USA) for providing the *bzip17/60* and *bzip28/60* double mutant seeds. We thank Prof. Wenqiang Tang (Hebei Normal University, China) for providing the *hsfa1-cq* mutant seeds. This work was supported by core funding from Temasek Life Sciences Laboratory and by Disruptive & Sustainable Technology for Agriculture Precision (DiSTAP), an interdisciplinary research group (IRG) of the Singapore MIT Alliance for Research and Technology (SMART) Center supported by the National Research Foundation (NRF), Prime Minister's Office, Singapore, under its Campus for Research Excellence and Technological Enterprise (CREATE) programme.

Author contributions

D.Z. and N.H.C. designed the experiments. D.Z. and H.Y.X. executed the experiments. D.Z. and N.H.C. wrote the manuscript.

Competing interests

The authors declare no competing interests.

Additional information

Supplementary information The online version contains supplementary material available at https://doi.org/10.1038/s41467-025-67909-9.

Correspondence and requests for materials should be addressed to Nam-Hai Chua.

Peer review information *Nature Communications* thanks the anonymous reviewer(s) for their contribution to the peer review of this work. A peer review file is available.

Reprints and permissions information is available at http://www.nature.com/reprints

Publisher's note Springer Nature remains neutral with regard to jurisdictional claims in published maps and institutional affiliations.

Open Access This article is licensed under a Creative Commons Attribution-NonCommercial-NoDerivatives 4.0 International License, which permits any non-commercial use, sharing, distribution and reproduction in any medium or format, as long as you give appropriate credit to the original author(s) and the source, provide a link to the Creative Commons licence, and indicate if you modified the licensed material. You do not have permission under this licence to share adapted material derived from this article or parts of it. The images or other third party material in this article are included in the article's Creative Commons licence, unless indicated otherwise in a credit line to the material. If material is not included in the article's Creative Commons licence and your intended use is not permitted by statutory regulation or exceeds the permitted use, you will need to obtain permission directly from the copyright holder. To view a copy of this licence, visit http://creativecommons.org/licenses/by-nc-nd/4.0/.

© The Author(s) 2025